Published in final edited form as:
J Chromatogr B Analyt Technol Biomed Life Sci. 2021 June 30; 1176: 122586. doi:10.1016/j.jchromb.2021.122586.

Erythrocyte haemotoxicity profiling of snake venom toxins after nanofractionation

Chunfang Xie[a,b], **Matyas A. Bittenbinder**[a,b,c], **Julien Slagboom**[a,b], **Arif Arrahman**[a,b], **Sven Bruijns**[d], **Govert W. Somsen**[a,b], **Freek J. Vonk**[a,b,c], **Nicholas R. Casewell**[e,f], **Juan J. García-Vallejo**[d], **Jeroen Kool**[a,b,*]

[a]Amsterdam Institute of Molecular and Life Sciences, Division of BioAnalytical Chemistry, Department of Chemistry and Pharmaceutical Sciences, Faculty of Science, Vrije Universiteit Amsterdam, De Boelelaan 1085, 1081HV Amsterdam, The Netherlands

[b]Centre for Analytical Sciences Amsterdam (CASA), 1098 XH Amsterdam, The Netherlands

[c]Naturalis Biodiversity Center, Darwinweg 2, 2333 CR Leiden, The Netherlands

[d]Department of Molecular Cell Biology and Immunology, Amsterdam Infection and Immunity Institute, Cancer Center Amsterdam, Amsterdam UMC, Vrije Universiteit Amsterdam, 1081 HZ Amsterdam, The Netherlands

[e]Centre for Snakebite Research and Interventions, Liverpool School of Tropical Medicine, Pembroke Place, Liverpool, L3 5QA, UK

[f]Centre for Drugs and Diagnostics, Liverpool School of Tropical Medicine, Pembroke Place, Liverpool, L3 5QA, UK

Abstract

Snakebite is classified as a priority Neglected Tropical Disease by the World Health Organization. Understanding the pathology of individual snake venom toxins is of great importance when developing more effective snakebite therapies. Snake venoms may induce a range of different pathologies, including haemolytic activity. Although snake venom-induced erythrocyte lysis is not the primary cause of mortality, haemolytic activity can greatly debilitate victims and contributes to systemic haemotoxicity. Current assays designed for studying haemolytic activity are not suitable for rapid screening of a large number of toxic compounds. Consequently, in this study, a high-throughput haemolytic assay was developed that allows profiling of erythrocyte lysis, and was validated using venom from a number of medically important snake species (*Calloselasma rhodostoma, Daboia russelii, Naja mossambica, Naja nigricollis* and *Naja pallida*). The assay was developed in a format enabling direct integration into nanofractionation analytics, which involves liquid chromatographic separation of venom followed by high-resolution fractionation and subsequent bioassaying (and optional proteomics analysis), and parallel mass spectrometric detection. Analysis of the five snake venoms via this nanofractionation approach involving haemolytic assaying provided venom-cytotoxicity profiles and enabled identification of the toxins responsible for haemolytic activity. Our results show that the elapid snake venoms (*Naja* spp.) contained both direct and indirect lytic toxins, while the viperid venoms (*C. rhodostoma* and *D.*

*corresponding author j.kool@vu.nl (J. Kool) Tel.: +31-20-598-7542.

Europe PMC Funders Author Manuscripts

russelii) only showed indirect lytic activities, which required the addition of phospholipids to exert cytotoxicity on erythrocytes. The haemolytic venom toxins identified were mainly phospholipases A_2s and cytotoxic three finger toxins. Finally, the applicability of this new analytical method was demonstrated using a conventional snakebite antivenom treatment and a small-molecule drug candidate to assess neutralisation of venom cytotoxins.

Keywords

Snakebite; venom; haemolytic toxins; nanofractionation analytics; erythrocytes haemolysis assay; proteomics analysis

1 Introduction

Snakebite is defined as a Neglected Tropical Disease (NTD) by the World Health Organization (WHO), with annual mortality ranging from 81,000 to 138,000 and morbidity rates surpassing 400,000 [1–3]. The regions in the world that are most heavily affected are the rural impoverished areas of the tropics and sub-tropics [3]. Despite its medical importance, snakebite remains systemically neglected by governments and public health communities [3]. Snake venoms consist of complex mixtures of proteins and peptides that vary between snake species and that are capable of causing various pathologies following envenoming, including neurotoxicity, haemotoxicity and cytotoxicity [3, 4]. Some of the most relevant toxin families found in snake venoms are phospholipases A_2s (PLA_2s), snake venom metalloproteinase (SVMPs), snake venom serine proteases (SVSPs) and three-finger toxins (3FTxs) [4–6]. Some of these toxins directly affect the haemostatic system and thus are capable of causing local and/or systemic haemorrhage. Haemostatic activities caused by such toxins include disruption of the vascular cell lining, inhibition or activation of clotting factors, vasodilation, inhibition of platelet aggregation or erythrocyte lysis [4, 5, 7, 8]. The latter comprises destruction of the erythrocyte membrane.

Erythrocyte lysis can result either from direct lysis or from indirect haemolysis. Indirect lysis requires the presence of phospholipids and is probably caused by disruption of the cell membrane by hydrolysis products of the phospholipids [9, 10]. Although snake venom-induced erythrocyte lysis seldom causes life-threatening pathology by itself, it may have a debilitating effect on snakebite victims and can be seen as one of the major contributing pathologies associated with haemotoxic activity [11–13]. Venom components that cause lysis by degradation of the erythrocyte membrane are considered direct lytic toxins and are only found in the venoms of elapid snakes, as opposed to the indirect lytic activities of viperid (vipers) snake venoms [14–16]. Previous studies have shown the requirement of exogenous phospholipids for haemolytic activity of PLA_2s found in viper venoms [14, 16, 17].

Standard haemolytic activity assays used for testing patient blood samples are not designed to enable rapid screening of a large number of cytotoxic compounds. Previous studies on haemolytic activity of snake venoms are mostly inefficient in terms of their limited throughput and resolution (i.e. time-consuming and laborious). In a recent study, however, Ramírez-Carreto *et al* performed a higher throughput haemolytic activity assay in 96-well

Europe PMC Funders Author Manuscripts

plate format to study the venom of a sea anemone for identification of pore-forming toxins [18]. In the study of Ramírez-Carreto *et al,* the toxin identification process involved elaborate purification steps prior to toxin identification. The development of a straightforward and miniaturized high-throughput screening (HTS) method based on high-density well plates that is combined with direct parallel toxin identification would be highly valuable for the study of haemolytic activity caused by snake venoms.

In this study, a HTS erythrocyte lysis assay was developed in 384-well plate format. As part of the assay development, various conditions, including the NaCl concentration of the assay medium, erythrocyte count and incubation time were optimized. In addition, the effects of surfactants on promoting erythrocyte lysis, and the potential cytotoxicity enhancing effects of phospholipids (egg yolk emulsions were used in this study) via facilitation of indirect lysis were assessed. The developed assay was then used for profiling haemolytic venom toxins using venom from five medically important snakes using nanofractionation analytics. This encompasses an integrated analytical approach in which venom toxins are separated by liquid chromatography (LC) and then fractionated in high resolution onto high density well plates (384-well plates were used in this study) for subsequent bioassaying. In parallel via a flow split, mass spectrometry (MS) data are measured from the LC effluent for toxin assignment purposes [19]. The content of wells containing venom toxins were also subjected to proteomics analysis to enable identification of the toxins responsible for the observed haemolytic activities. We demonstrate that the developed assay can be used for profiling venom-induced haemolysis and for providing characteristic erythrocyte cytotoxicity profiles of individual toxins found in crude snake venoms.

2 Experimental

2.1 Materials

Water was purified with a Milli-Q Plus system (Millipore, Amsterdam, The Netherlands). The HPLC grade acetonitrile (ACN) and formic acid (FA) were purchased from Biosolve (Valkenswaard, The Netherlands). NaCl, Trisodium citrate dihydrate, Tween-20, Triton X-100, egg yolk, Ficoll, Trypan blue and Dulbecco's phosphate buffered saline (PBS) were purchased from Sigma-Aldrich (Zwijndrecht, The Netherlands). Varespladib (A-001) and marimastat (also purchased from Sigma-Aldrich) were dissolved in DMSO (≥ 99.9%, Sigma-Aldrich) to a concentration of 10 mM prior to store at –20 °C. For assaying, these stocks were diluted in 0.5% NaCl in water to desired concentrations. Snake venom pools sourced from *Calloselasma rhodostoma* (captive bred, Thailand ancestry), *Daboia russelii* (Sri Lanka), *Naja mossambica* (Tanzania), *Naja nigricollis* (Nigeria) and *Naja pallida* (Tanzania) were lyophilized and provided by the Centre for Snakebite Research and Interventions, Liverpool School of Tropical Medicine (UK). The lyophilised venoms were dissolved into water to a concentration of 5.0 ± 0.1 mg/mL and stored at –80 °C. Prior to use, each venom solution was diluted in water to the defined concentrations in this study. Monospecific equine $F(ab')_2$-based Malayan pit viper antivenom used in this study for cytotoxicity neutralisation tests of *Calloselasma rhodostoma* venom, was from the Queen Saovabha Memorial Institute, The Thai Red Cross Society (Bangkok, Thailand).

2.2 High-resolution nanofractionation of snake venoms

Venoms were separated by LC followed by parallel MS detection and nanofractionation using a post-column split. A Waters XBridge reversed-phase C18 column (250 × 4.6 mm, packed with 3.5 μm porous particles) was used and maintained at 30 °C using a Shimadzu CTO-30A column oven. The total solvent flow rate was 0.5 mL/min, controlled by two Shimadzu LC-30AD parallel pumps. Mobile phase A was composed of 98% H_2O, 2% ACN and 0.1% FA, while mobile phase B was 98% ACN, 2% H_2O and 0.1% FA. Gradient elution was performed as follows: a linear increase of mobile phase B from 0% to 50% in the first 20 min, followed by another 4 min from 50% to 90%, then kept at 90% for 5 min, subsequently mobile phase B was decreased from 90% to 0% in 1 min and kept at 0% for 10 min for re-equilibration. For each analysis, 50 μL venom solution was injected by a Shimadzu SIL-30AC autosampler. The column effluent was split into a 1:9 ratio. The 10% fraction was sent to a Shimadzu SPD-M20A Prominence diode array detector (UV detector) and then optionally to MS detection (Impact II QTOF, Bruker Daltonics, Billerica, MA, USA) packed with an electrospray ionization source operated in positive-ion mode. The 90% fraction was sent to a fraction collector. This was either a commercially available FractioMate™ nanofractionator (SPARK-Holland & VU, Netherlands, Emmen & Amsterdam) controlled by FractioMator software (Spark-Holland, The Netherlands, Emmen) or a modified Gilson 235P autosampler controlled by in-house developed Ariadne software. The fractions were collected at a resolution of 6 s/well onto transparent 384-well plates (F-bottom, rounded square well, polystyrene, without lid, clear, non-sterile; Greiner Bio One, Alphen aan den Rijn, The Netherlands). The well plates with collected fractions were subsequently dried overnight using a Christ Rotational Vacuum Concentrator (RVC 2–33 CD plus, Zalm en Kipp, Breukelen, The Netherlands) operated at –80 °C with help of a cooling trap. The dried plates were stored at –20 °C until bioassaying.

2.3 Isolation of red blood cells from whole blood

Red blood cells were isolated from multiple healthy donor-derived buffy coats (Sanquin, Amsterdam). Erythrocyte isolation was performed at room temperature. The 50 mL collected blood was citrated and diluted in 130 mL PBS-1% citrate solution and mixed gently (without shaking). The PBS-1% citrate solution was prepared by dissolving trisodium citrate dihydrate in PBS solution. After diluting, 30 mL of the citrated blood was pipetted into a 50 mL tube containing 15 mL Ficoll solution. This tube was subsequently centrifuged for 30 min at 700×g (no brakes, acc=4, dec=1) using an Allegra™ X-12 Centrifuge (Beckman Coulter). After centrifuging, the blood was separated as three layers; the top layer consisting of plasma, the middle layer containing mono nuclear cells and the bottom layer consisting of erythrocytes. The bottom layer was pipetted into a new 50 mL tube for further washing. The erythrocytes were washed three times with 50 ml 0.9% NaCl solution (with in-between centrifuging for 10 min at 700×g (no brakes, acc=4, dec=1)) and then re-suspended in 0.9% NaCl solution (1:10, v/v). Cell counts were determined by cellular staining with trypan blue followed by cell counting in duplicate using a Bürker counting chamber. By using the determined cell counts, the erythrocytes could be diluted to desired cell counts during assay optimisation.

2.4 Erythrocyte lysis assay

The erythrocyte lysis assay was based on measuring the absorbance of erythrocyte suspensions at 540 nm by a platereader in 384-well plate format. Erythrocyte lysis was detected as an increase in absorbance of the erythrocyte suspensions, after allowing non-lysed erythrocytes to settle (cell lysis results in red coloration of the upper clear solution). During the first stage of assay development, the effects of the erythrocyte count, the NaCl solution concentration and the incubation time were investigated on assay performance in Eppendorf tube format. The stock erythrocyte suspension was diluted in NaCl solutions of different concentrations (0.0, 0.1, 0.2, 0.3, 0.4, 0.5, 0.6, 0.7, 0.8 and 0.9%) to total volumes of 1 mL (in 1.5 ml Eppendorf tubes) to generate suspensions with different erythrocyte counts, varying between 0.6, 1.5, 3.0 and 6.0 ($\times 10^7$)/mL. During the incubations conducted in Eppendorf tubes, 50 μL aliquots were taken from the upper layers of the settling cellular suspensions at different time points (0, 10, 20, 30, 45 or 60 min) and were transferred to the wells of a 384-well plate for final platereader measurement. After 60 min, the suspensions were centrifuged (30 s at 805×g; 2000 rpm) to allow full sedimentation of all erythrocytes before transferring the last supernatants to the 384-well plate. The optimal NaCl concentration is the lowest NaCl concentration that produces an osmotic pressure in the cells under which they stay intact during the course of the experiment. This concentration of NaCl results in the erythrocytes having the least stability and hence largest vulnerability to lysis when in presence of haemolytic venom toxins. The optimal incubation time is the shortest time needed for all non-lysed erythrocytes to fully settle (and thus not interfere with the eventual platereader measurement).

Next, the optimal erythrocyte count, NaCl concentration and incubation time were used for subsequent assay development fully conducted in 384-well plates containing nanofractionated cytotoxic venom toxins. For this, 50 μL of diluted erythrocyte suspension was pipetted at room temperature by a Multidrop™ 384 Reagent Dispenser (Thermo Fisher Scientific, Ermelo, The Netherlands) onto 384-well plates containing vacuum centrifuged venom fractions (see Section 2.2: High-resolution nanofractionation of snake venoms). The erythrocyte suspensions in these plates were then incubated at room temperature under a 75 degree angle that allows settling of erythrocytes on one side of each well in the plates in order to prevent interference with the subsequent platereader absorbance measurements. This way an increase in absorbance can be associated with erythrocyte lysis resulting in an increase in red coloration (and not with settled intact erythrocytes at the bottom of each well). After the incubation step, the absorbance of each well was measured on a Varioskan™ Flash Multimode Reader (Thermo Fisher Scientific, Ermelo, The Netherlands) at a wavelength of 540 nm at 25 °C. Haemolytic activity was then depicted as bioactivity chromatograms by plotting the absorbance of each well versus the chromatographic retention time for each fraction collected. The last parameters to be investigated for assay development included testing the effects of the surfactants Triton X-100 and Tween-20 on facilitating erythrocyte lysis, and the effect of egg yolk for studying indirect lysis by cytotoxins that require the presence of phospholipids to exert their cytotoxicity.

Europe PMC Funders Author Manuscripts

2.5 Inhibiting effects of varespladib, marimastat and antivenom on venom-induced lytic activity

Following assay development and integration into nanofractionation analytics, the inhibitory effects of the PLA_2 inhibitor varespladib, the SVMP inhibitor marimastat and species-specific antivenom on lytic activity was investigated for several of the venoms under study, for proof-of-concept demonstration of the utility of the assay. For this, 5 μL volumes of various concentrations of varespladib solutions (resulting in final assay concentrations of 20, 4 and 0.8 μM), 5 μL volumes of a marimastat solution (resulting in a final assay concentration of 20 μM) or 5 μL volumes of an antivenom solution (directly taken from Malayan pit viper antivenom vial) were added to all wells of freeze-dried 384-well plates (5 μL volumes of a 0.5% NaCl solution were added to venom-only control plates). For each solution, one well plate with nanofractionated venom toxins was used. For these bioassay pipetting steps, a VWR Multichannel Electronic Pipette was used. Directly after pipetting the solutions, plates were centrifuged for 1 min at 805 × *g* (2000 rpm) using a 5810 R centrifuge (Eppendorf, Germany) followed by pre-incubation for 30 min at room temperature. Meanwhile, the erythrocyte lysis assay solutions were prepared as described above (Section 2.4) of which 45 μL volumes were added to the plates after the pre-incubation step. This was then followed by assay incubation and platereader measurement as described above (Section 2.4). All analyses were performed in at least duplicate.

2.6 Correlation of biological data to MS and proteomics data

In one of our previous studies [19], venoms of the snake species *C. rhodostoma* and *D. russelii,* which were included in this study, were analysed using the nanofractionation approach with parallel MS detection, which yielded accurate molecular masses of eluting venom toxins and their coagulopathic activities. In addition, proteomics data was acquired after in-well tryptic digestion followed by nanoLC-MS/MS analysis of the contents of the wells. Using the data acquired, the UniprotKB database was searched with Mascot for information on the toxin class and possible known functions of the toxins under study. Correlation of the LC-UV data for the venoms acquired in the present study with the LC-UV data obtained in the previous study, allowed for the bioassay data from the present study to be correlated with the MS and proteomics data obtained from the previous study [19]. For the venoms of the snake species *N. mossambica, N. nigricollis* and *N. pallida*, of which no MS and proteomics data was available from the nanofractionation analytics approach, the same procedure as described by Slagboom *et al.* [19] was used to acquire similar datasets.

3 Results and Discussion

Haemolysis caused by snake envenoming may result in secondary kidney damage or renal failure [20–22]. Erythrocyte lysis can be the result of the action of various cytotoxins and haemotoxins [7, 11, 14, 16]. Important classes of haemolytic snake venom toxins include cytotoxic PLA_2s, cytotoxic 3FTxs, SVMPs, L-amino acid oxidase, C-type lectins and hyaluronidases [23, 24]. Cytotoxins have also previously been sub-classified based on their specific cellular activity, such as myotoxins, cardiotoxins and generic cytotoxins, though few studies have assessed the generality of their mechanisms of action [3, 23, 25]. This study describes the development and application of a low-volume 384-well plate format assay

for assessing haemolytic activity that was integrated into a high-throughput screening and nanofractionation analytics pipeline. First, the haemolysis assay was optimised by varying the NaCl concentration, erythrocyte count and incubation time, followed by assessment of the effects of surfactants and the assay's capability of measuring indirect lytic activity by incorporating phospholipids (i.e. egg yolk). Following optimisation, the assay was combined with nanofractionation analytics to profile venoms from five haemolytic snakes, specifically: *C. rhodostoma*, *D. russelii*, *N. mossambica*, *N. nigricollis* and *N. pallida*. Snake venoms were separated by LC followed by nanofractionation analytics with post-column haemolytic activity assessment next to parallel LC-MS and proteomics-based venom toxin identification. The resulting data were used to identify haemolytic toxin components from the venoms of the five medically important snake species.

3.1 Development of the erythrocyte lysis assay

The erythrocyte lysis assay performance was first investigated by diluting washed and re-suspended erythrocytes into NaCl solutions of different concentration. Incubation of this first set of experiments was performed in Eppendorf tubes, permitting straightforward sampling from the upper layers of the tubes containing settling erythrocytes for subsequent transfer to well plates for eventual platereader measurement. The goal here was to evaluate the stability of erythrocytes to the different NaCl concentrations tested, and to evaluate the effect of different incubation times. The optimal NaCl concentration was determined as the lowest concentration of NaCl that did not result in cell lysis by osmosis. This concentration is expected to have the erythrocytes in a surrounding where they are least stable and hence most prone to venom-induced lysis. All incubations were conducted in Eppendorf tubes from which at different time points, aliquots were taken from the upper layers of the settling cellular suspensions and were transferred to wells in a well plate for final platereader measurement. Lysed cells result in red coloration, which is measured by the platereader. To simultaneously assess the effect of cell sedimentation, aliquots were taken at different time points. The results obtained are shown in Figure 1a. During incubation, slowly the erythrocytes settled and depending on the NaCl concentration, erythrocyte lysis was observed as the result of osmotic pressure, indicated by a change in supernatant colour. The resulting absorbance of the supernatants (i.e. around 1.0 at 540 nm) did not change significantly at NaCl concentrations ranging from 0.0% to 0.4%, while a clear concentration-response was observed from 0.5% to 0.9% NaCl. These results indicate that erythrocytes lysed quickly (directly at the start of the incubation period) at NaCl concentrations ranging from 0.0% to 0.4%, as evidenced by plateau of absorbance over time. Additionally, no sedimented erythrocytes were observed at the end of the experiment for these NaCl concentrations, indicating complete cellular lysis. At NaCl concentrations ranging from 0.5% to 0.9%, the erythrocytes did not lyse but slowly sedimented resulting in a decrease in absorbance (i.e. yielding clear top layers in each Eppendorf tube) over time and sedimented erythrocytes were observed clearly at the end of the experiment. Photographic images of the erythrocytes at the end of the experiment revealed a correlation between NaCl concentration and erythrocytes morphology (or lysis for the lower NaCl concentrations) (see Supporting Information, Section S1). At NaCl concentrations ranging between 0.5% to 0.9%, a high average absorbance (over 2.0) was observed at the beginning of the experiment, due to erythrocytes observed in suspension in the top layer of the

Eppendorf tubes. During the time frame of the experiment, erythrocytes slowly settled, resulting in a time-dependent decrease in supernatant absorbance. The optimal incubation time is the time required for all non-lysed erythrocytes to fully settle (and thus not interfere with the eventual platereader measurement). After 60 min incubation, all Eppendorf tubes were centrifuged (ensuring full settlement of all erythrocytes) followed by acquiring the last aliquot for measurement (i.e. the "after centrifugation" readings displayed in Figure 1a) from each tube. As mentioned above, optimal conditions were met at a NaCl concentration of 0.5% and an incubation time of (at least) 60 min, in which the average absorbance measured was close to the average absorbance of the aliquots measured after the final centrifugation step. This indicated that an incubation time of 60 min was appropriate as no significant increase in erythrocyte sedimentation occurred thereafter, and was confirmed visually with similar red erythrocyte sediment at the 60 min incubation time point and after centrifugation.

Next, measurements were performed with different erythrocyte counts using the defined 60 min incubation time. As observed in Figure 1b, full erythrocyte lysis was observed at NaCl concentrations ranging from 0.0% to 0.4% for all erythrocyte counts tested at these NaCl concentrations. As a result, the supernatant absorbances were found to increase linearly with erythrocyte count. For the higher NaCl concentrations tested, absorbances decreased drastically at concentrations of NaCl of 0.5% and higher (similar to the previous experiment described, see Figure 1a). For all subsequent assays described in this study, an erythrocyte count of 3.0×10^7/mL was used as it gave a good assay window at an acceptable erythrocyte counts. The results of all measurements performed during this assay optimization step (i.e. the effect of all tested concentrations of NaCl in combination with all erythrocyte counts tested, at all tested incubation times) are provided in the Supporting Information (Section S2).

The optimisation experiments yielded erythrocyte assay conditions with an erythrocyte count of 3.0×10^7/mL, a NaCl concentration of 0.5% and an incubation time of 60 min. These conditions were next transferred to full 384-well plate format (i.e. both the incubation and the readout are performed in 384-well plate format). For this, onto 384-well plates containing (optionally freeze-dried) samples (such as nanofractionated and vacuum-centrifuged venom toxins in the wells), 50 μL of a suspension of erythrocytes with a count of 3.0×10^7/mL in 0.5% NaCl was pipetted into all wells by robotic pipetting. Then, the plates were incubated for 60 min under an angle of 75 degrees at 25 °C, which was followed by final readout in platereader format at 540 nm.

This assay format was now integrated into nanofractionation analytics and used for cytotoxic venom profiling. Each of the five medically-important snake venoms ((concentration of 5.0 mg/mL) was analysed by LC and nanofractionated on well plates, followed by application of the erythrocyte lysis assay to the fractions. The venoms of the spitting cobras *N. mossambica*, *N. nigricollis* and *N. pallida* showed clear erythrocyte lysis activity, visualised as positive peaks in the bioactivity chromatograms, while the venoms of *C. rhodostoma* and *D. russelii* did not show any notable cytotoxic activity (Figure 2). After measurement, erythrocytes lysis was also clearly visible (by visible inspection) in bioactive wells containing cytotoxins from *N. mossambica*, *N. nigricollis* and *N. pallida* venoms. A typical

photographic image of one of these 384-well plates, and photographs with discussions on the visual inspection of the cellular morphology of the erythrocytes by microscopy, together with duplicate bioactivity chromatogram results, are shown in the Supporting Information (Section S3).

Next, the venoms of *N. mossambica*, *N. nigricollis* and *N. pallida* were tested over a concentration range (1.0, 2.0, 3.0, 4.0 and 5.0 mg/mL) using the nanofractionation approach, to investigate dose-response effects (Figure 3). As anticipated, lower venom concentrations resulted in decreased areas of the lysis peaks of the bioactivity chromatogram, indicating reduced erythrocyte lysis. At the highest venom concentrations tested, however, similar cytotoxicity peaks were observed due to full lytic activity of all erythrocytes was attained at these concentrations tested. As erythrocyte lysis measured for these three snake venoms was still clearly visible at a venom concentration of 1.0 mg/mL, this concentration was used for further experiments. All described nanofractionation experiments were conducted at least in duplicate, and duplicate bioactivity chromatograms are shown in the Supporting Information (Section S4).

3.2 Secondary optimization of the erythrocyte lysis assay

Subsequent optimization of the erythrocyte lysis bioactivity assay following integration with nanofractionation analytics was performed by studying the effect of small differences in NaCl concentration (i.e. 0.45%, 0.50%, 0.55%, 0.60% and 0.65%) using an erythrocyte count of 3.0×10^7/mL in combination with *N. pallida* venom at a concentration of 1.0 mg/mL. The results obtained from these analyses are shown in Figure 4 and the duplicate bioactivity chromatograms of these experiments are displayed in the Supporting Information (Section S5). At 0.45% NaCl, a large portion of the erythrocytes lysed in all wells due to osmotic pressure and resulted in high background absorbance (see insert panel, top left of Figure 4). This resulted in a reduction in erythrocyte number available for lysis in wells with nanofractionated lytic venoms toxins and, in turn, resulted in a lower lytic activity peak and high levels of background noise in the bioactivity chromatograms. At NaCl concentrations between 0.50% and 0.60%, the majority of erythrocytes in wells not containing cytotoxic venom toxins remained viable during the measurement period, and post-measurement microscopy analysis revealed that increasing NaCl concentrations resulted in enhanced shrinking of the erythrocytes. In other words, the higher NaCl concentration resulted in a decrease of the susceptibility of the erythrocytes for lysis by cytotoxic venom toxins. In Figure 4, this is observed by the single cytotoxic peak (retention time of 16.5 min) that decreased in intensity upon increasing NaCl concentrations. At the highest concentration tested (i.e. 0.65% NaCl), no lytic activity was observed. From these results, we concluded the optimal NaCl concentration was 0.50%, and this was used thereafter as the final assay concentration.

Next, the effect of the surfactants Triton X-100 and Tween-20 on facilitating erythrocyte lysis was studied with *N. pallida* venom. Detergents or surfactants are known to interfere with cell membranes, disrupting the lipid bilayer [26, 27] by solubilising membrane proteins and thereby increasing membrane permeability [27]. The non-ionic detergent Triton X-100 is an alkylphenoxy-polyethoxy surfactant which is able to disrupt biological membranes

by inducing a phase transition from membrane lamellae to mixed protein-lipid-detergent micelles [28, 29]. Tween-20 is a non-ionic surfactant which is reported to contribute to cell wall collapse [30], to remove proteins from the membrane surface [31], and to influence the membrane lipid composition and the membrane fluidity [32]. The surfactants may destabilise erythrocytes, hence making them more viable for lytic activity, thereby increasing assay sensitivity. Both Triton X-100 and Tween-20 are also potential agents that can render an increase in phospholipid solubility (such as the egg yolk used in this assay as emulsion). Upon increasing the concentration of Triton X-100 or Tween-20, erythrocyte stability against lytic venom activity indeed was found to decrease for both surfactants tested, as observed by a concentration-dependent increase in the positive lytic activity (as indicated by the peak at 16.5 min in Figure 5). However, at the highest concentration tested (i.e. 0.1 mg/mL for Triton X-100 and 1.0 mg/mL for Tween-20), most erythrocytes were found to have lysed directly (see the high background signals in the insert panels, top left of Figures 5a and 5b). This evidently prevents lysis from being measured in wells containing cytotoxic venom toxins. Our results confirmed that both Triton X-100 and Tween 20 could potentially be used as agents that increase assay sensitivity. The duplicate bioactivity chromatograms of these experiments are provided in the Supporting Information (Section S6).

Next, the effect of egg yolk on facilitating indirect lysis of erythrocytes was investigated on both viper (*C. rhodostoma* and *D. russelii*) and elapid (*Naja* spp.) venoms. Without the addition of egg yolk (as described earlier in Figure 2), no lytic activity was observed for the two viper venoms, whereas a sharp lysis peak was observed for each of three elapid venoms. By adding egg yolk, the lytic activity profile (observed as positive peaks) for all venoms under study was increased in a concentration-response manner (Figure 6). Egg yolk concentration-dependent increases in lytic activity were observed at retention times of ~20 min for *C. rhodostoma* venom and ~18 min for *D. russelii* venom. A similar concentration-dependent pattern was observed when the egg yolk concentration was increased for the elapid venoms. However, upon increasing the egg yolk concentration for all three elapid venoms tested, a second bioactivity peak (at ~20 min) appeared adjacent to the one already visible without the addition of egg yolk addition (at ~16.5 min) (Figure 6). At the highest concentrations of egg yolk tested, baseline fluctuations were found to increase, while the total observed lytic activity in the bioactivity chromatograms slightly decreased. Taking these observations into consideration, an optimal egg yolk emulsion concentration of 1.75 mg/mL was selected. The duplicate bioactivity chromatograms of these experiments are provided in the Supporting Information (Section S7).

Although the haemolytic activity observed in the snake venoms under study is not thought to play a major role in overall venom lethality, it can be considered a manifestation of pathophysiological relevance [11, 13]. A previous study by Condrea *et al.* [14, 16] showed that PLA_2s isolated from elapid venom were capable of hydrolysing phospholipids, whereas those isolated from viper venoms could not, unless exogenous phospholipids were added. Indirect haemolysis can be activated by adding exogenous phospholipids to venom phospholipases [16, 33]. Egg yolk consists of lipids and proteins, of which ~50% are phospholipids, which thus could be used to induce indirect lytic activity [34–36]. Indeed, egg yolk has been used previously to study the indirect haemolytic activity of snake venoms and was reported to enable lysis by hydrolytic activity of PLA_2s in viper venoms [16, 17,

37]. Our results here show clear increases in total venom-induced lytic activity for both viper and elapid venoms following the addition of increasing amounts of egg yolk.

3.3 Identification of haemolytic venom toxins

Haemolytic toxins were identified by correlating the positive cytotoxic erythrocytes lysis peaks with acquired MS and proteomics data which were (i) previously measured by Slagboom *et al.* [19] for *C. rhodostoma* and *D. russelii* venoms and (ii) measured in this study under the same experimental conditions as Slagboom *et al.* for the venoms of *N. mossambica, N. nigricollis* and *N. pallida.* The obtained results are displayed in Table 1. For the toxins of which no exact mass data could be acquired by LC-MS (e.g. for toxins in the higher mass range such as SVSPs), only proteomics data obtained from the Mascot searches is provided. For the two viper venoms under study, PLA_2s were the main cytotoxic toxins identified, whereas for the three elapid venoms studied, 3FTxs were the major cytotoxic toxin type in addition to PLA_2s. It has to be noted that unambiguously assigning single toxins to each detected bioactivity peak, especially when the peak is broad, is quite challenging, due to multiple toxins closely co-eluting. An additional caveat is that despite venom toxins generally being stable, some venom toxins might have (partly) denatured upon exposure to the LC eluent and thereby lost their activity.

3.4 Inhibitory effects of antivenom and the small molecule snakebite treatment candidates varespladib and marimastat on venom-induced erythrocyte lysis.

As final proof-of-concept of the capability of the developed erythrocyte lysis assay, we investigated the inhibitory effects of conventional treatment (antivenom) and the new small molecule-based treatment candidates varespladib and marimastat on nanofractionated cytotoxins. First, we explored neutralisation of *C. rhodostoma* venom toxins using a species-specific antivenom. As anticipated, the observed lytic activity in the bioactivity chromatogram (sharp peak at 20.0 min in Figure 7a) of nanofractionated *C. rhodostoma* venom was fully inhibited by this antivenom at the tested concentration. Next, the inhibitory capability of varespladib on venom-induced erythrocyte lysis caused by the venoms of *N. mossambica*, *N. nigricollis* and *N. pallida* was explored (Figure 7b). Varespladib is a broad-range PLA_2 inhibitor known for its capability of neutralising pathological snake venom PLA_2s [38–40], and African spitting cobra venoms (i.e. the *Naja* species under study) are known to contain considerable abundances of PLA2s, which seemingly contribute to venom cytotoxicity [41, 42] (Table 1). Broad peaks showing haemolytic activities were observed in the bioactivity chromatograms of each of the three investigated venoms in the venom-only control experiments. The addition of varespladib resulted in only a limited, though visible, reduction in venom activity (Figure 7b). The intensity of the positive lytic activity peaks for *N. mossambica* and *N. nigricollis* venoms were dose-dependently reduced, though only limited lytic inhibition was achieved at the highest concentration tested (i.e. 20 μM). For *N. pallida* venom, the tailing part of the single bioactivity peak observed was very slightly reduced, at a varespladib concentration of 0.8 μM varespladib, but the addition of increasing concentrations of varespladib failed to confer additional inhibition. From Table 1 it can be seen that for the *Naja* venoms both cytotoxic 3FTxs and PLA_2s were found as bioactives. As varespladib is not capable of neutralising the 3FTxs, these findings are consistent with other studies that suggest that cytotoxic 3FTxs are the primary cytotoxins responsible for

the majority of cell lysis caused by the venoms of spitting cobras (and their near relatives) [42–44]. As a control experiment, we also used marimastat (which is a broad range SVMP inhibitor) at a concentration of 20 μM, to assess its inhibitory capability against *N. pallida* venom (results of this experiment can be found in the Supporting Information Figure S13). As anticipated, no inhibition was observed as marimastat is a metalloprotease inhibitor and no SVMPs are involved in cytotoxicity of *N. pallida* venom. All duplicate bioactivity chromatograms of the experiments shown in this section are provided in the Supporting Information (Section S8).

4 Conclusion

This study describes the development and application of a high-throughput erythrocyte lysis assay in 384-well plate format. The assay protocol developed relies on absorbance measurement of the red coloration of the medium after lysis of erythrocytes. In order to prevent measurement interferences from settling erythrocytes, plate incubation was conducted under an angle of 75 degrees outside the platereader. This way, non-lysed erythrocytes settled to the sides of the wells thereby not forming a red precipitation layer over the complete bottom of each well, through which the absorbance measurements were finally performed in platereader format. This way, cellular lysis resulting in change in coloration could be measured as positive signal. For the optimised assay, a total volume of 50 μl assay medium, containing 0.5% NaCl and 1.75 mg/mL egg yolk emulsion in water, was added to each well by robotic pipetting. To this medium, erythrocytes were suspended to a count of 3.0×10^7/mL, and after an incubation time of 60 min at 75 degrees angle at 25 °C, the final readout in platereader format at 540 nm was performed. The developed assay was then integrated into nanofractionation analytics and the platform was used for further fine-tuning of the assay using venoms of the medically important snakes *C. rhodostoma, D. russelii, N. mossambica, N. nigricollis* and *N. pallida.*The elapid snake venoms (*Naja* spp.) showed both direct and indirect lytic activities, while the viperid venoms (*C. rhodostoma* and *D. russelii*) only showed indirect lytic activities which required the addition of phospholipids (i.e. egg yolk) to exert cytotoxicity on erythrocytes. The venoms under study were profiled and the resulting cytotoxic peaks observed were correlated with parallel acquired MS and proteomics data in order to identify the cytotoxic venom components in these venoms. The results showed PLA_2s and 3FTxs were the major toxins contributing to the haemolytic activity observed. In a final proof-of-concept experiment, we demonstrated the value and future applicability of the described methodology for investigating the efficacy of current and new snakebite therapies at neutralising snake venom cytotoxins.

Supplementary Material

Refer to Web version on PubMed Central for supplementary material.

Acknowledgements

C.X. is funded by a China Scholarship Council (CSC) fellowship (201706250035). N.R.C. acknowledges support from a UK Medical Research Council (MRC) Research Grant (MR/S00016X/1) and Confidence in Concept Award (CiC19017), and a Sir Henry Dale Fellowship (200517/Z/16/Z) jointly funded by the Wellcome Trust and Royal

Society. Special thanks go to Dr. H.F.G. Heijnen from the Lab Clinical Chemistry & Haematology, University Medical Center Utrecht, the Netherlands, for valuable discussions on assay development and haemotoxicity in general.

References

1. Longbottom J, et al. Vulnerability to snakebite envenoming: a global mapping of hotspots. The Lancet. 2018; 392 (10148) 673–684.
2. Williams DJ, et al. Strategy for a globally coordinated response to a priority neglected tropical disease: Snakebite envenoming. PLoS neglected tropical diseases. 2019; 13 (2) 7059–7080.
3. Gutiérrez JM, et al. Snakebite envenoming. Nature reviews Disease primers. 2017; 3 (1) 1–21.
4. Slagboom J, et al. Haemotoxic snake venoms: their functional activity, impact on snakebite victims and pharmaceutical promise. British journal of haematology. 2017; 177 (6) 947–959. [PubMed: 28233897]
5. Sajevic T, Leonardi A, Križaj I. Haemostatically active proteins in snake venoms. Toxicon. 2011; 57 (5) 627–645. [PubMed: 21277886]
6. Xiong S, Huang C. Synergistic strategies of predominant toxins in snake venoms. Toxicology letters. 2018; 287: 142–154. [PubMed: 29428543]
7. Matsui T, Fujimura Y, Titani K. Snake venom proteases affecting hemostasis and thrombosis. Biochimica et biophysica acta. 2000; 1477: 146–56. [PubMed: 10708855]
8. Lu Q, Clemetson J, Clemetson KJ. Snake venoms and hemostasis. Journal of Thrombosis and Haemostasis. 2005; 3 (8) 1791–1799. [PubMed: 16102046]
9. Fletcher JE, et al. Comparison of a relatively toxic phospholipase A_2 from Naja nigricollis snake venom with that of a relatively non-toxic phospholipase A2 from Hemachatus haemachatus snake venom—II: Pharmacological properties in relationship to enzymatic activity. Biochemical pharmacology. 1980; 29 (11) 1565–1574. [PubMed: 7396987]
10. Stoykova S, et al. Hemolytic activity and platelet aggregation inhibitory effect of vipoxin's basic $sPLA_2$ subunit. Interdisciplinary Toxicology. 2013; 6 (3) 136–140. [PubMed: 24678250]
11. Braud S, Bon C, Wisner A. Snake venom proteins acting on hemostasis. Biochimie. 2000; 82 (9-10) 851–859. [PubMed: 11086215]
12. Hati R, et al. Snake venom hemorrhagins. Critical reviews in toxicology. 1999; 29 (1) 1–19. [PubMed: 10066158]
13. Condrea, E. Snake venoms. Springer; 1979. 448–479.
14. Condrea E, et al. Susceptibility of erythrocytes of various animal species to the hemolytic and phospholipid splitting action of snake venom. Biochimica et Biophysica Acta (BBA)-Specialized Section on Lipids and Related Subjects. 1964; 84 (4) 365–375.
15. Aloof-Hirsch S, De Vries A, Berger A. The direct lytic factor of cobra venom: purification and chemical characterization. Biochimica et Biophysica Acta (BBA)-Protein Structure. 1968; 154 (1) 53–60.
16. Condrea E, De Vries A, Mager J. Hemolysis and splitting of human erythrocyte phospholipids by snake venoms. Biochimica et Biophysica Acta (BBA)-Specialized Section on Lipids and Related Subjects. 1964; 84 (1) 60–73.
17. De Vries A, et al. Hemolytic action of indirect lytic snake venom in vivo. Toxicon. 1962; 1 (1) 19–23.
18. Ramírez-Carreto S, et al. Identification of a pore-forming protein from sea anemone Anthopleura dowii Verrill (1869) venom by mass spectrometry. Journal of Venomous Animals and Toxins including Tropical Diseases. 2019; 25
19. Slagboom J, et al. High throughput screening and identification of coagulopathic snake venom proteins and peptides using nanofractionation and proteomics approaches. PLoS Neglected Tropical Diseases. 2020; 14 (4) e0007802 [PubMed: 32236099]
20. Vikrant S, Jaryal A, Parashar A. Clinicopathological spectrum of snake bite-induced acute kidney injury from India. World J Nephrol. 2017; 6 (3) 150–161. [PubMed: 28540205]
21. Dharod MV, et al. Clinical predictors of acute kidney injury following snake bite envenomation. North American journal of medical sciences. 2013; 5 (10) 594–599. [PubMed: 24350071]

22. Chugh KS, et al. Acute renal failure following poisonous snakebite. American Journal of Kidney Diseases. 1984; 4 (1) 30–38. [PubMed: 6741936]
23. Chakrabarty, D, Sarkar, A. Snake Venoms. Inagaki, H, , et al., editors. Springer; Netherlands: Dordrecht: 2017. 327–342.
24. Hiu JJ, Yap MKK. Cytotoxicity of snake venom enzymatic toxins: phospholipase A_2 and l-amino acid oxidase. Biochemical Society Transactions. 2020; 48 (2) 719–731. [PubMed: 32267491]
25. Gutiérrez, JMa; Ownby, CL. Skeletal muscle degeneration induced by venom phospholipases A2: insights into the mechanisms of local and systemic myotoxicity. Toxicon. 2003; 42 (8) 915–931. [PubMed: 15019491]
26. Tsuchido T, et al. Lysis and aberrant morphology of Bacillus subtilis cells caused by surfactants and their relation to autolysin activity. Antimicrobial agents and chemotherapy. 1990; 34 (5) 781–785. [PubMed: 2113794]
27. Partearroyo MA, et al. Surfactant-induced cell toxicity and cell lysis: a study using B16 melanoma cells. Biochemical pharmacology. 1990; 40 (6) 1323–1328. [PubMed: 2403386]
28. Gurtubay J, et al. Triton X-100 solubilization of mitochondrial inner and outer membranes. Journal of bioenergetics and biomembranes. 1980; 12 (1-2) 47–70. [PubMed: 7410344]
29. Prado A, et al. Membrane-surfactant interactions The effect of triton X-100 on sarcoplasmic reticulum vesicles. Biochimica et Biophysica Acta (BBA)-Biomembranes. 1983; 733 (1) 163–171. [PubMed: 6224512]
30. Seo D-J, Fujita H, Sakoda A. Structural changes of lignocelluloses by a nonionic surfactant, Tween 20, and their effects on cellulase adsorption and saccharification. Bioresource technology. 2011; 102 (20) 9605–9612. [PubMed: 21852116]
31. Hoffman WL, Jump AA. Tween 20 removes antibodies and other proteins from nitrocellulose. Journal of immunological methods. 1986; 94 (1-2) 191–196. [PubMed: 3782811]
32. Li J, et al. Temperature-and surfactant-induced membrane modifications that alter Listeria monocytogenes nisin sensitivity by different mechanisms. Appl Environ Microbiol. 2002; 68 (12) 5904–5910. [PubMed: 12450809]
33. Turner JC. Absence of lecithin from the stromata of the red cells of certain animals (ruminants), and its relation to venom hemolysis. Journal of Experimental Medicine. 1957; 105 (3) 189–193. [PubMed: 13406178]
34. Palacios LE, Wang T. Egg-yolk lipid fractionation and lecithin characterization. Journal of the American Oil Chemists' Society. 2005; 82 (8) 571–578.
35. Slotta, KH, Gonzalez, J, Roth, S. The direct and indirect hemolytic factors from animal venoms. RUSSELL Animal Toxins; Elsevier; Amsterdam, The Netherlands: 2016. 369–377.
36. Al-Abdulla IH, Sidki AM, Landon J. An indirect haemolytic assay for assessing antivenoms. Toxicon. 1991; 29 (8) 1043–1046. [PubMed: 1949062]
37. Martins L, et al. In vitro hemolytic activity of Bothrops lanceolatus (fer-de-lance) venom. Journal of Venomous Animals and Toxins including Tropical Diseases. 2009; 15 (3) 498–508.
38. Lewin M, et al. Varespladib (LY315920) appears to be a potent, broad-spectrum, inhibitor of snake venom phospholipase A2 and a possible pre-referral treatment for envenomation. Toxins. 2016; 8 (9) 248–263.
39. Bryan-Quirós W, et al. Neutralizing properties of LY315920 toward snake venom group I and II myotoxic phospholipases A_2 . Toxicon. 2019; 157: 1–7. [PubMed: 30447275]
40. Wang Y, et al. Exploration of the inhibitory potential of varespladib for snakebite envenomation. Molecules. 2018; 23 (2) 391–403.
41. Petras D, et al. Snake venomics of African spitting cobras: toxin composition and assessment of congeneric cross-reactivity of the pan-African EchiTAb-Plus-ICP antivenom by antivenomics and neutralization approaches. J Proteome Res. 2011; 10 (3) 1266–80. [PubMed: 21171584]
42. Kazandjian TD, et al. Convergent Evolution of Pain-Inducing Defensive Venom Components in Spitting Cobras. bioRxiv. 2020. 2020.07.08.192443
43. Troiano J, Gould E, Gould I. Hemolitic action of Naja naja atra cardiotoxin on erythrocytes from different animals. Journal of Venomous Animals and Toxins including Tropical Diseases. 2006; 12 (1) 44–58.

44. Condrea E. Membrane-active polypeptides from snake venom: cardiotoxins and haemocytotoxins. Experientia. 1974; 30 (2) 121–129. [PubMed: 4592382]

Europe PMC Funders Author Manuscripts

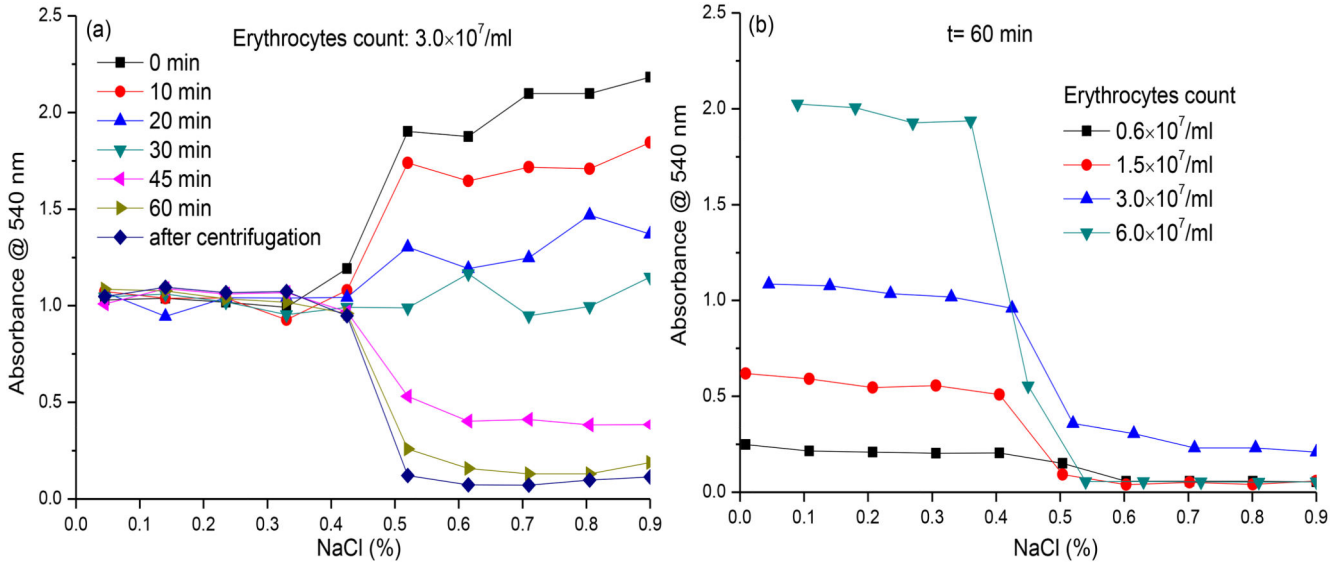

Figure 1. Absorbance of top layers of erythrocyte suspensions measured at different NaCl concentrations, erythrocyte counts and incubation times.

a) Absorbance measured at different incubation times using a NaCl concentration between 0 to 0.9%; b) Absorbance measured after a 60 min incubation time for different erythrocyte counts using a NaCl concentration between 0 to 0.9%.

Europe PMC Funders Author Manuscripts

Europe PMC Funders Author Manuscripts

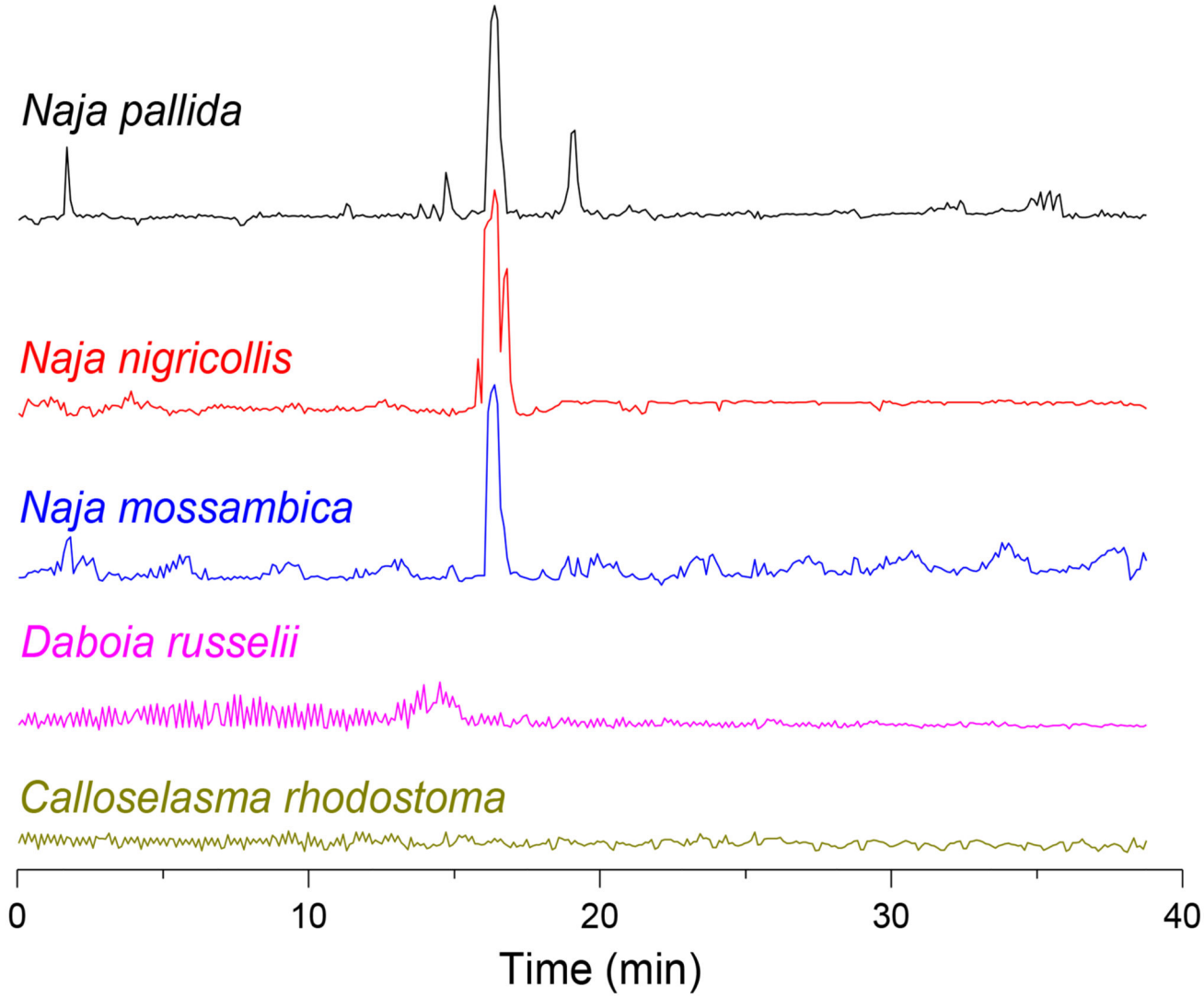

Figure 2.

Erythrocytes lysis bioactivity chromatograms resulting from nanofractionated venoms of *C. rhodostoma, D. russelii, N. mossambica, N. nigricollis* and *N. pallida* (venom concentration of 5.0 mg/mL). Positive peaks in the chromatograms indicate erythrocyte lysis activity.

Europe PMC Funders Author Manuscripts

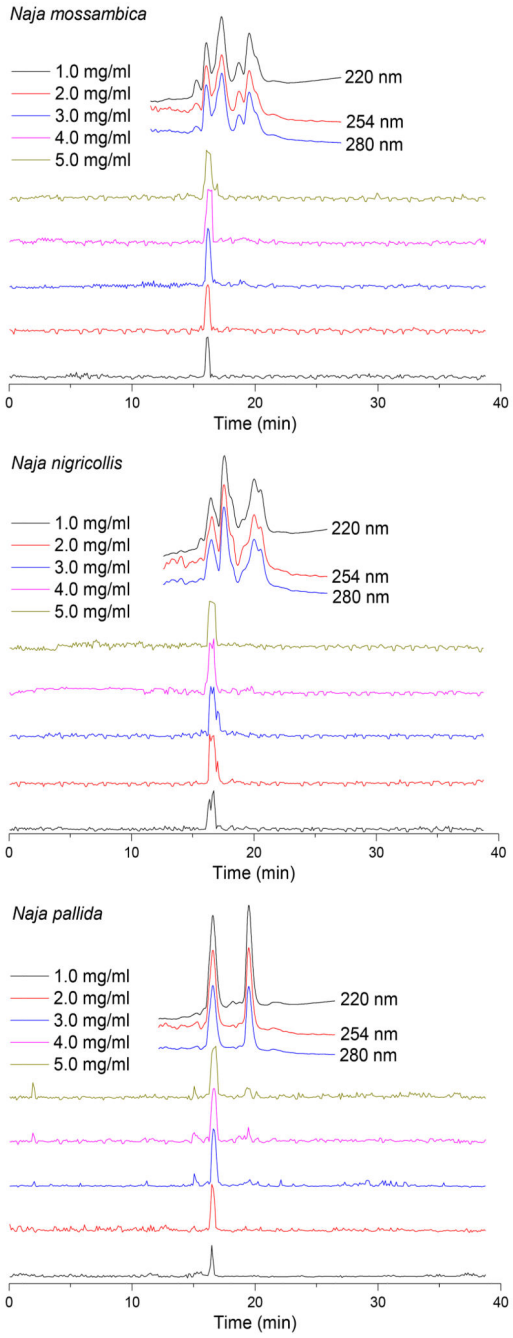

Figure 3.

Superimposed erythrocyte lysis bioactivity chromatograms resulting from assaying nanofractionated venoms of *N. mossambica*, *N. nigricollis* and *N. pallida* analysed at venom concentrations of 1.0, 2.0, 3.0, 4.0 and 5.0 mg/mL. The top superimposed chromatograms are characteristic profiles of UV traces measured at 220, 254 and 280 nm.

Europe PMC Funders Author Manuscripts

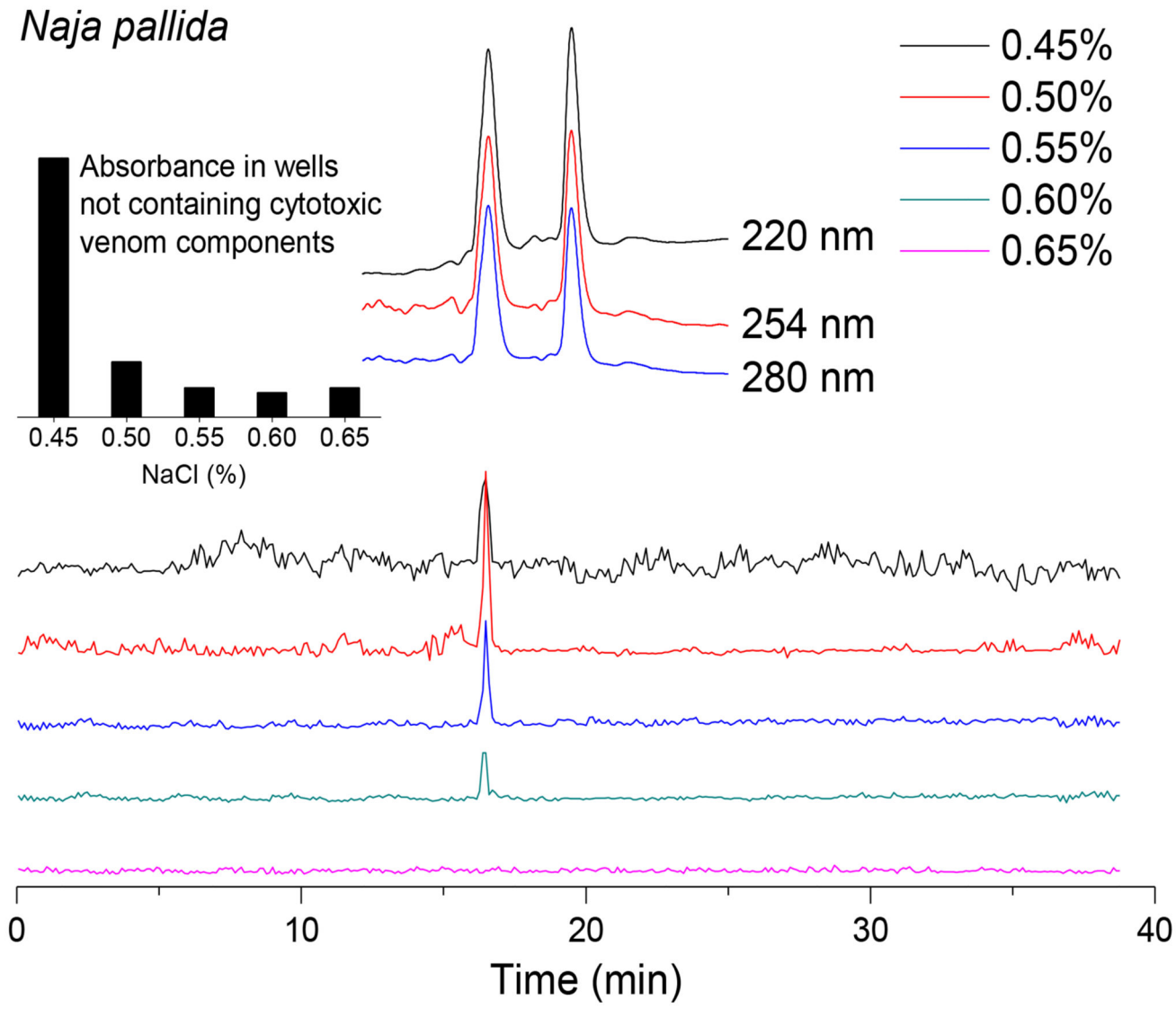

Figure 4.

Bioactivity chromatograms of nanofractionated venom from *N. pallida* (venom concentration of 1.0 mg/mL) resulting from optimisation experiments with different NaCl assay concentrations. The inserted bar graph shows the absorbance in wells not containing cytotoxic venom components, tested under these different NaCl concentrations. The top superimposed chromatograms are characteristic profiles of UV traces measured at 220, 254 and 280 nm.

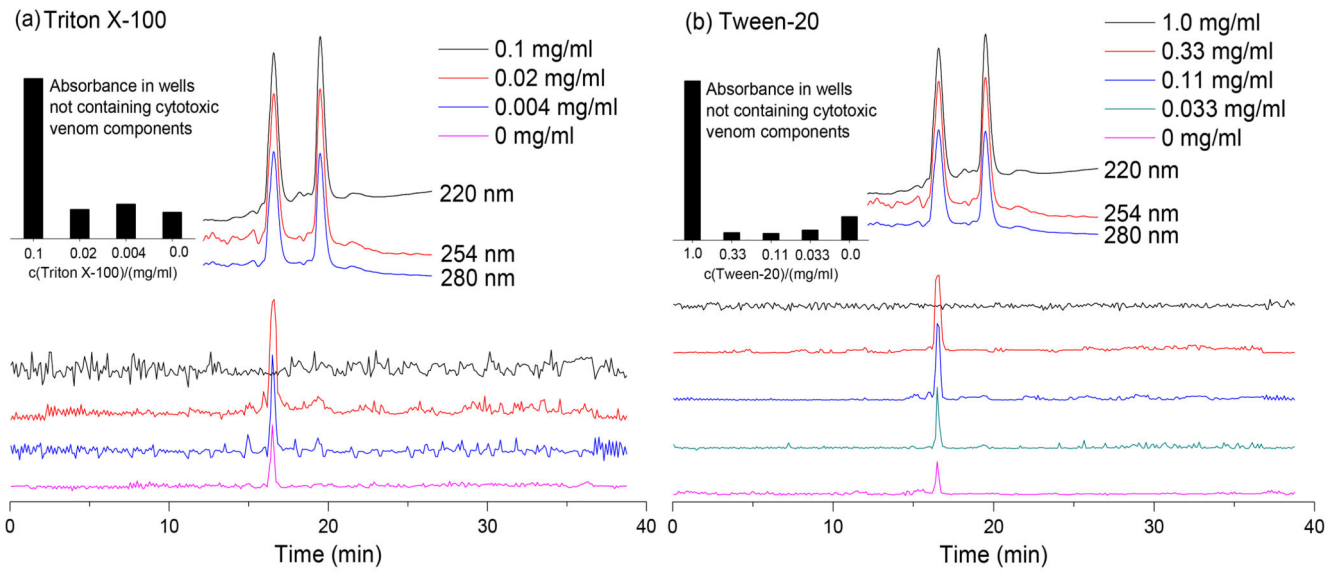

Figure 5. Effect of various concentrations of surfactants on venom-induced erythrocyte lysis

(a) Triton X-100, and (b) Tween-20. Surfactants were tested on nanofractionated toxins from *N. pallida* venom (1.0 mg/mL). The insert bar graph shows absorbance in wells not containing cytotoxic venom components, tested under different concentrations of the surfactants. The top superimposed chromatograms are characteristic profiles of UV traces measured at 220, 254 and 280 nm.

Europe PMC Funders Author Manuscripts

Europe PMC Funders Author Manuscripts

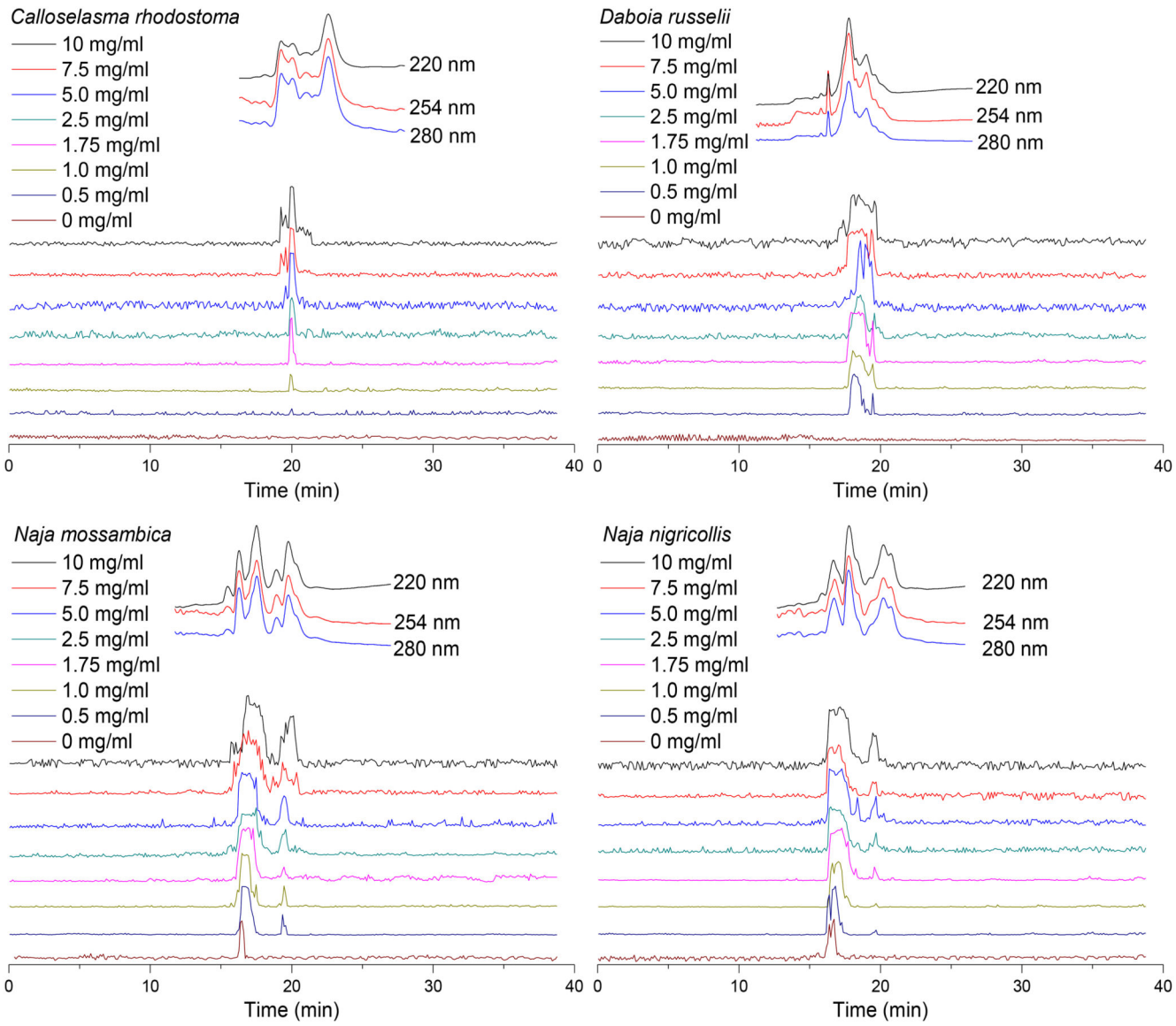

Figure 6.

The effect of egg yolk on erythrocyte lysis activity caused by nanofractionated *C. rhodostoma, D. russelii, N. mossambica, N. nigricollis* and *N. pallida* venoms (1.0 mg/ml). Egg yolk concentrations ranged from 0 to 10 mg/mL. The top superimposed chromatograms are characteristic profiles of UV traces measured at 220, 254 and 280 nm.

Europe PMC Funders Author Manuscripts

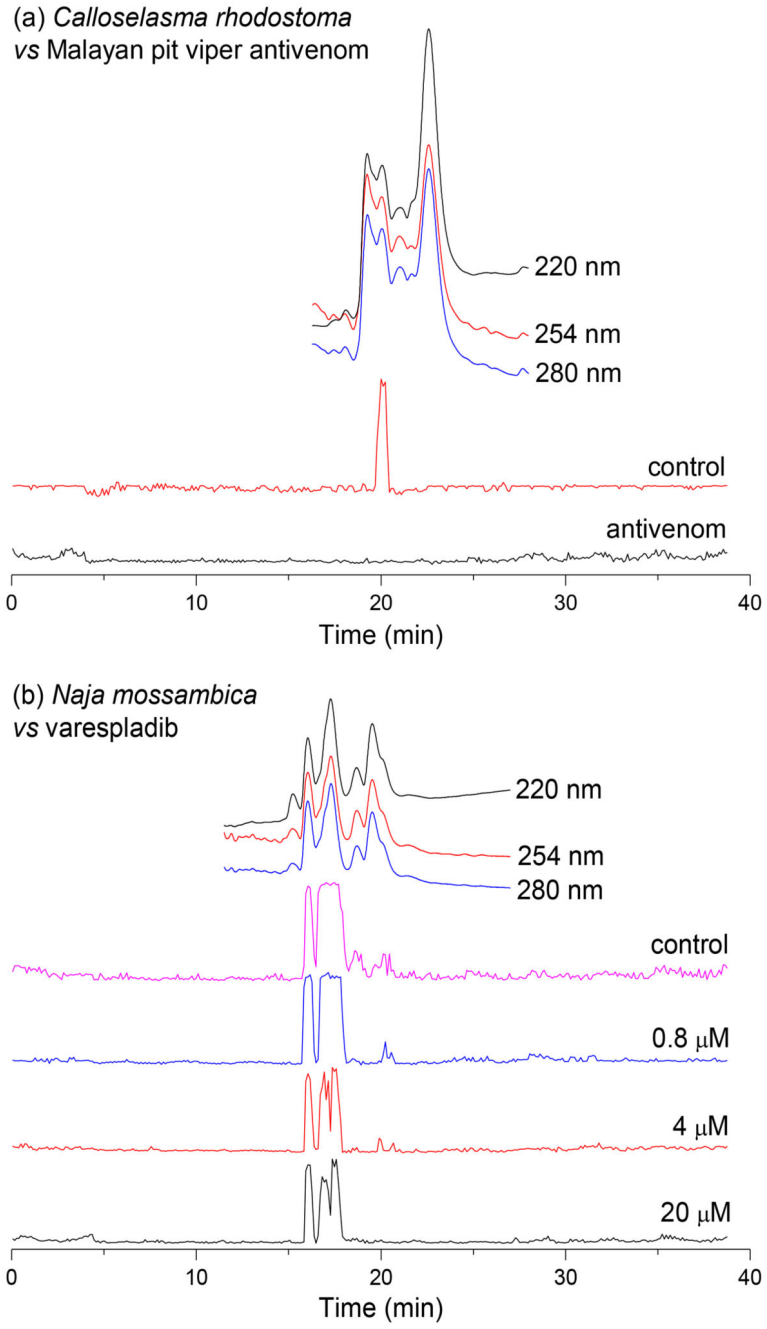

Figure 7.

The inhibiting effects of (a) Malayan pit viper antivenom on *C. rhodostoma* venom-induced erythrocyte lysis activity, (b) varespladib on venom-induced erythrocyte lysis activity caused by *N. mossambica*, *N. nigricollis* and *N. pallida* venoms. All venoms were nanofractionated at a 1.0 mg/mL concentration, and inhibitor concentrations are displayed in the figures. The top superimposed chromatograms are characteristic profiles of UV traces measured at 220, 254 and 280 nm.

Table 1
Correlated MS and proteomics data matching haemolytic venom toxins

Peak retention times are adapted from Figure 6; PLA_2 = phospholipase A_2; SVSP = snake venom serine protease; CTL = C-type lectin; 3FTx = three-finger toxin; HI toxin = haemostasis impairing toxin; PAI toxin = platelet aggregation inhibiting toxin). The toxins identified with high protein scores (i.e. >1,000) for each cytotoxicity retention time frame are highlighted with a grey background.

Species	Peak retention time (min)	Mascot results matching the exact mass	Exact mass from MS data	Exact mass calculated from Mascot data	Toxin class	Protein score	Described activity
C.rhodostoma	19.3-20.5	PA2BD_CALRH	13665.1	13665	PLA_2	3082	**Myotoxin**
	19.3-20.5	SLEB_CALRH	-	15190	CTL	1785	**HI toxin PAI toxin**
	19.3-20.5	VSPF1_CALRH	-	26570	SVSP	1027	**HI toxin**
	19.3-20.5	PA2AB_CALRH	-	15141	PLA_2	447	**HI toxin PAI toxin**
	19.3-20.5	VSPF2_CALRH	-	29145	SVSP	339	**HI toxin**
	19.3-20.5	SLEA_CALRH	-	15962	CTL	276	**HI toxin PAI toxin**
D.russelii	16.9-19.8	PA2B3_DABRR	-	13687	PLA_2	3612	**Unknown**
	16.9-19.8	PA2B8_DABRR	13587.2	13587	PLA_2	3549	**Myotoxin**
	16.9-19.8	PA2B5_DABRR	-	13587	PLA_2	3252	**Unknown**
N. mossambica	15.6-18.4	3SA2_NAJMO	6797.2	6787	3FTx	3257	**Cytotoxin**
	15.6-18.4	PA2A1_NAJMO	-	14008	PLA_2	1624	**Myotoxin**
	15.6-18.4	PA2B2_NAJMO	-	14023	PLA_2	1557	**HI toxin Myotoxin**
	15.6-18.4	3SA5_NAJMO	6834.3	6832	3FTx	1469	**Cytotoxin**
	15.6-18.4	3SA3_NAJMO	6882.3	6881	3FTx	1219	**Cytotoxin**
	15.6-18.4	3SA1_NAJMO	6815.2	6813	3FTx	1197	**Cytotoxin**
	15.6-18.4	3SA4_NAJMO	6705.3	6702	3FTx	215	**Cytotoxin**
	15.6-18.4	PA2B3_NAJMO	13279.6	13278	PLA_2	369	**Myotoxin**
	19.1-20.5	3SA1_NAJMO	6815.2	6813	3FTx	2228	**Cytotoxin**
	19.1-20.5	PA2A1_NAJMO	-	14008	PLA_2	135	**Myotoxin**
N. nigricollis	16.0-18.6	3SAN_NAJNG	6883.3	6882	3FTx	3211	**Cardiotoxin**
	16.0-18.6	PA2B4_NAJNG	13245.8	13244	PLA_2	2973	**HI toxin**
	19.1-20.4	3SAN_NAJNG	6883.3	6882	3FTx	1617	**Cardiotoxin**
	19.1-20.4	WAPN_NAJNG	-	5748	3FTx	675	**Unknown**
N. pallida	14.9-18.7	3SA1 NAJPA	-	7279	3FTx	3103	**Cytotoxin**
	14.9-18.7	PA2B_NAJPA	13321.7	13316	PLA_2	555	**HI toxin**
	14.9-18.7	3S11_NAJPA	6785.1	6782	3FTx	414	**Neurotoxin**
	18.8-19.9	3SA1_NAJPA	-	7279	3FTx	4742	**Cytotoxin**
	18.8-19.9	PA2B_NAJPA	13321.7	13316	PLA_2	206	**HI toxin**